Impact of Spin-up Forcing on Vegetation States Simulated by a Dynamic Global Vegetation Model Coupled with a Land Surface Model

LI Fang* (李 芳), ZENG Xiaodong[1] (曾晓东), SONG Xiang[1,2] (宋 翔),

TIAN Dongxiao[1,2] (田东晓), SHAO Pu[1,2] (邵 璞), and ZHANG Dongling[1] (张东凌)

[1]*Institute of Atmospheric Physics, Chinese Academy of Sciences, Beijing* 100029

[2]*Graduate University of Chinese Academy of Sciences, Beijing* 100049

ABSTRACT

A dynamic global vegetation model (DGVM) coupled with a land surface model (LSM) is generally initialized using a spin-up process to derive a physically-consistent initial condition. Spin-up forcing, which is the atmospheric forcing used to drive the coupled model to equilibrium solutions in the spin-up process, varies across earlier studies. In the present study, the impact of the spin-up forcing in the initialization stage on the fractional coverages (FCs) of plant functional type (PFT) in the subsequent simulation stage are assessed in seven classic climate regions by a modified Community Land Model's Dynamic Global Vegetation Model (CLM-DGVM). Results show that the impact of spin-up forcing is considerable in all regions except the tropical rainforest climate region (TR) and the wet temperate climate region (WM). In the tropical monsoon climate region (TM), the TR and TM transition region (TR-TM), the dry temperate climate region (DM), the highland climate region (H), and the boreal forest climate region (BF), where FCs are affected by climate non-negligibly, the discrepancies in initial FCs, which represent long-term cumulative response of vegetation to different climate anomalies, are large. Moreover, the large discrepancies in initial FCs usually decay slowly because there are trees or shrubs in the five regions. The intrinsic growth timescales of FCs for tree PFTs and shrub PFTs are long, and the variation of FCs of tree PFTs or shrub PFTs can affect that of grass PFTs.

Key words: vegetation, initial condition, spin-up forcing, Dynamic Global Vegetation Model, Land Surface Model

1. Introduction

The terrestrial biosphere, as an important component of the land surface, plays a pivotal and active role in the climate system through biophysical interactions and biogeochemical exchanges with other components of the climate system (Foley et al., 1996; Betts et al., 1997; Cramer et al., 2001; Sitch et al., 2003; Dai et al., 2004; Bonan, 2008). A coupled model of the dynamic global vegetation model (DGVM) and the land surface model (LSM), such as CLM-DGVM (Levis et al., 2004a; Zeng et al., 2008; Oleson et al., 2008),

MOSES-TRIFFID (Essery et al., 2001; Cox, 2001), CLASS-CTEM (Arora, 2003), ORCHIDEE (Krinner et al., 2005), CoLM-VEGAS (Liu, 2007), ED-JULES (Fisher, 2008), and CoLM-DGVM (Chen, 2008), can integrate more realistic biophysical, biogeographical, biogeochemical, and dynamic vegetation processes of the land surface into a single and physically consistent framework than an LSM or a DGVM alone can. On the one hand, the coupled model can simulate the transient variation of vegetation states rather than adopting prescribed vegetation states in an LSM. On the other hand, it provides more accurate water and heat

---

conditions than the simple biophysical module in a DGVM does. The coupled model aims to simulate the interaction between land surface and atmosphere on a global scale, and has been a primary member of an earth system model which is the major approach of current global change studies.

A physically-consistent initial condition of the coupled model is difficult to derive from observations. The initial condition of the coupled model generally includes vegetation composition; the number of individuals; height of canopy top and bottom; crown area; leaf area index; grams of carbon in leaves, roots, sapwoods, and above and below ground litter; soil moisture; temperature of lake, soil, snow, vegetation, and ground; emitted infrared radiation; snow interface depth; canopy and snow water; and so on. In addition to the intrinsic observational error, the observational data for most of the above-mentioned variables is unavailable on a global scale (Qian et al., 2006).

Therefore, a coupled model of DGVM and LSM is generally initialized by a spin-up process. During the spin-up process, the model starts from a specified initial state and is driven by atmospheric forcing which is named spin-up forcing. Until simulated carbon pools and vegetation coverage between two neighboring years with the same atmospheric forcings are nearly the same, the equilibrium solutions of the initialization variables listed above compose the physically-consistent initial condition of the coupled model (Bonan and Levis, 2006). Since the spin-up process for a coupled model of DGVM and LSM includes the adjustment process of slow carbon pools and the vegetation succession process, its spin-up time for a global simulation is generally hundreds of years and longer than the spin-up time for an LSM with prescribed vegetation states (Yang et al., 1995; Dai et al., 2003; Rodell et al., 2005).

Various spin-up forcings have been used in earlier studies. Due to a lack of long-term observed atmospheric data, spin-up forcings are generally artificially constructed. The most commonly used spin-up forcings are derived by cycling the observed atmospheric data for a year (Zeng et al., 2005; Köhler et al., 2005; Morales et al., 2007; Liu, 2007; Chen, 2008; Cook et al., 2008; Zeng et al., 2008) or for a multiyear period (Kim and Wang, 2005; Bonan and Levis, 2006; Liang and Xie, 2008) repeatedly. In addition, the atmospheric data obtained by looping through climatology data is also used as the spin-up forcing for DGVMs (Foley et al., 1996; Kucharik et al., 2000; Sato et al., 2007) and LSMs with prescribed vegetation states (Rodell et al., 2005).

So far, the selection of spin-up forcings for initializing the coupled model has been arbitrary. Whether the arbitrary selection will influence the vegetation simulation in the subsequent stage is unclear. In the present study, an ensemble of 42 simulations is made by a coupled model of LSM and DGVM. The specifications of these simulations are identical except for the spin-up forcing. The standard deviation of the 42 simulations is used to assess the impact of spin-up forcing in the initialization stage on vegetation simulation in the subsequent simulation stage. Simulations in seven classic climate regions are used to replace 42 global simulations in order to reduce computation load, though the coupled model is mainly used for global simulation. Obviously, for regions where spin-up forcing affects simulation strongly, the impact of spin-up forcing must be considered for parameter adjustment in model development and for interpretation of physical processes that one wishes to study.

To generalize plant function to a global scale, DGVMs represent vegetation as plant functional types (PFTs) instead of species. Each PFT is represented by an average individual plant with biomass, crown area, height, stem diameter, individual population, and fractional coverage of the population in a grid cell (Bonan et al., 2003). Different PFTs have different optical properties of leaves and stems which determine reflection, transmittance, and absorption of solar radiation; root distribution parameters which control the uptake of water from soil; aerodynamic parameters which determine resistance to heat, moisture, and momentum transfer; and photosynthetic parameters which determine stomatal resistance, photosynthesis, and transpiration (Zeng, 2001; Bonan et al., 2002b). In this paper, for simplicity, only the fractional coverages (FCs) of plant functional types (PFTs) are investigated. FC of PFT is the primary vegetation-state variable in a PFT-based coupled model of DGVM and LSM (Bonan and Levis, 2006; Zeng et al., 2008; Zeng, 2010). It describes the vegetation composition and affects boundary momentum, carbon, water, energy fluxes by assigning weights to relative variables calculated at the PFT sub-grid level (Foley et al., 1996; Zeng, 2001; Bonan et al., 2002a; Sitch et al., 2003; Levis et al., 2004a).

In section 2, the modified Community Land Model's DGVM (CLM3.0-DGVM) and atmospheric forcing dataset are introduced briefly. Then the methodology concerning the region selection and experimental design are described in section 3. section 4 analyzes the impact of spin-up forcing in the initialization stage on FCs in subsequent simulation stage. Finally, concluding remarks and discussions are given

in section 5.

2. Model and data

2.1 *Model*

CLM3.0-DGVM is one of the most widely used coupled models of DGVM and LSM in current climate research (Levis et al., 2004a; Bonan and Levis, 2006). In this coupled model, DGVM offers CLM3.0 information about vegetation composition, structure, and phenology. In turn, CLM3.0, as a biogeophysics module, offers DGVM information about water and heat states and gross primary production (GPP). The biogeochemistry module includes litter and soil biogeochemistry process as well as autotrophic respiration. Both biogeophysics and biogeochemistry modules are calculated at each model time step. Plant phenology is updated daily. The vegetation dynamics module is calculated at the end of each year, and the major processes, listed in calculation order, are reproduction, turnover, mortality due to negative net primary production (NPP), allocation, competition, background mortality and mortality due to stress, natural fire disturbances, survival, and establishment processes. The model represents spatial heterogeneity in land cover by dividing each grid cell into five columns representing different land cover types with prescriptive percent coverage: glacier, lake, wetland, urban, and vegetation. The vegetation column is further divided into several non-overlapping patches of PFTs. In the model, only natural vegetation can be simulated, and vegetation is represented by the carbon stored in leaves, roots, sapwood, and heartwood. Given the carbon pools, the model can derive FC and other vegetation state variables.

The CLM3.0-DGVM revised by Zeng et al. (2008) and Zeng (2010) (hereafter simply called CLM-DGVM) is used as model platform in this study. CLM-DGVM incorporates CLM3.0-DGVM with a sub-model for temperate and boreal shrubs, as well as other revisions such as the "two-leaf" scheme for photosynthesis and the definition of fractional coverage of PFTs. By adding temperate and boreal shrubs which are absent in CLM3.0-DGVM, the model now has 12 PFTs, including 7 tree PFTs, 3 grass PFTs, and 2 shrub PFTs (Table 1). Zeng (2010) showed that CLM-DGVM reduced the bias of the original CLM3.0-DGVM by increasing the tree coverage and decreasing grass coverage and by producing a more realistic ratio of evergreen to deciduous trees in the tropical and boreal regions. The geographic distribution of its vegetation simulation was in good agreement with the CLM4.0 surface data which were based on a range of MODIS, AVHRR, and climate products. In addition,

Table 1. Plant functional types (PFTs) in CLM-DGVM.

PFT	Abbreviation
Trees	
Broadleaf Evergreen Tropical	BET Tropical
Broadleaf Deciduous Tropical	BDT Tropical
Broadleaf Evergreen Temperate	BET Temperate
Needleleaf Evergreen Temperate	NET Temperate
Broadleaf Deciduous Temperate	BDT Temperate
Needleleaf Everegreen Boreal	NET Boreal
Broadleaf Deciduous Boreal	BDT Boreal
Grasses	
C4	——
C3 Non-arctic	——
C3 Arctic	——
Shrubs	
Broadleaf Deciduous Temperate	BDS Temperate
Broadleaf Deciduous Boreal	BDS Boreal

CLM-DGVM can correctly simulate the dependence of vegetation distribution on climate conditions. In CLM-DGVM, ecosystem changed from desert to shrubland then to grassland and, finally, to forest as mean annual precipitation increased, and changed from cold desert to boreal shrubland then to coexistence of grassland/forest and, finally, to hot desert as mean annual temperature increased. Furthermore, the dominant PFT changed from boreal to temperate to tropical, accompanying with the changes in leaf trait and phenology type, as annual temperature and precipitation increased. These results agreed with standard ecological theory.

2.2 *Forcing Data*

The atmospheric dataset for 1960–1999 with three-hourly (0000, 0300, 0600 UTC, etc.) and T62 resolution constructed by Qian et al. (2006) is used as the forcing data for the CLM-DGVM. The variables include precipitation, surface air temperature, specific humidity, wind speed, air pressure, and downward solar radiation.

In this dataset, the monthly station records are used to correct the spurious long- term changes and biases in the six-hourly NCEP–NCAR reanalysis precipitation, surface air temperature, and solar radiation fields. The surface specific humidity from the reanalysis dataset is adjusted using the adjusted surface air temperature and original relative humidity from the reanalysis data. Surface wind speed and air pressure are interpolated directly from the NCEP–NCAR reanalysis data.

3. Methodology

3.1 *Region selection*

In the present study, seven classic climate regions are selected: the tropical rainforest climate region (TR), the tropical monsoon climate region (TM), the TR and TM transition region (TR-TM), the wet temperate climate region (WM), the dry temperate climate region (DM), the highland climate region (H), and the boreal forest climate region (BF) (Fig. 1). The criteria for region selection are mainly based on the updated Köppen-Geiger climate classification system (Peel et al., 2007), but with precipitation and temperature data described in the section 2.2. Table 2 describes the locations and defining criteria of these regions in detail. Because a single grid cell may exhibit unique characteristics, we choose three grid cells in each climate region to ensure general regional representation.

3.2 *Experimental design*

An ensemble of 42 offline simulations is made by CLM-DGVM in each climate region, whose discrepancy in FCs is analyzed here. All simulations are forced by the same observed atmospheric data from 1960 to 1999. The 42 simulations are different only in initial conditions, which are derived as follows.

In the initialization stage, CLM-DGVM starts from a bare ground scenario (no plants present) and is driven by various spin-up forcings. The 42 spin-up forcings are separated into three sets as described in
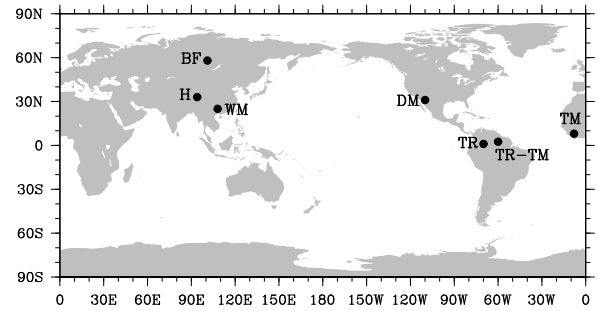

Fig. 1. Geographical locations of seven classic climate regions selected in the present paper.

Table 3. The first set (S1) has 40 atmospheric forcings. Each uses the repetition of one-year atmospheric observations from 1960 to1999 covering different climate conditions from wet to dry, and from warm to cold. Set 2 (S2) uses the climatological mean instead to generate an initial condition under normal climate conditions. Here, the climatology is the temporal mean of observational data from 1960 to 1999 at each time step. In set 3 (S3), the whole period of observed data is cycled through the spin-up process. Due to the interannual variability of climate (which is absent in both S1 and S2), the S3 simulations usually need a longer spin-up time. The corresponding equilibrium states provide a wide range of initial conditions based on commonly used spin-up forcings.

In the spin-up process, the period for the ecosystem to approach an equilibrium state varies with location and with spin-up forcing. In TR, the periods are 50

Table 2. Description of seven classic climate regions selected in the present study and their defining criteria and locations.

Region name	Defining criteria*	Location
Tropical rainforest climate region (TR)	$T_{cold} \geqslant 18°C$; $P_{dry} \geqslant 60$ mm m^{-1}	Amazon rainforest region (0°–1.9°N, 66.6°–72.2°W)
TR and TM transition region (TR-TM)	$T_{cold} \geqslant 18°C$; $P_{dry} \geqslant 100-MAP/25$	Northeastern Amazon Basin (1.9°–3.8°N, 57.2°–62.8°W)
Tropical monsoon climate region (TM)	$T_{cold} \geqslant 18°C$; 60 mm m$^{-1} > P_{dry} \geqslant$ 100–MAP/25	West African Monsoon region (6.7°N, 11.2°W), (8.6°N, 13.1°W), (8.6°N, 11.2°W)
Wet temperate climate region (WM)	$T_{hot} > 10°C$ & $0 < T_{cold} < 18°C$; MAP$\geqslant 10 \times P_{threshold}$	East Asian Monsoon region (24.8°–26.7°N, 105.9°–111.6 °E)
Dry temperate climate region (DM)	$T_{hot} > 10°C$ & $0 < T_{cold} < 18°C$; MAP$< 10 \times P_{threshold}$	Southwestern North America (30.5°–32.4°N, 107.8°–113.4°W)
Highland climate region (H)	$E > 3000$ m & $-18°C < MAT < 10°C$	South Tibet Plateau (32.4°–34.3°N, 90.9°–96.6°E)
Boreal forest climate region (BF)	$T_{cold} \leqslant 0°C$ & $T_{hot} > 10°C$ MAP$\geqslant 10 \times P_{threshold}$	South Russia (57.1°–59.0°N, 98.4°–104.1°E)

Note: *MAP=mean annual precipitation, MAT=mean annual temperature, T_{hot}=temperature of the hottest month, T_{cold}=temperature of the coldest month, P_{dry}=precipitation of the driest month, $P_{threshold}$=varies according to the following rules (if 70% of MAP occurs in winter then $P_{threshold}=2 \times MAT$, if 70% of MAP occurs in summer then $P_{threshold}=2 \times MAT+28$, otherwise $P_{threshold}=2 \times MAT+14$). Summer (winter) is defined as the warmer (cooler) six-month period of AMJJAS (ONDJFM), E=elevation.

Table 3. Description of three sets of spin-up atmospheric forcings and their spin-up time in the spin-up process to construct the various initial conditions of CLM-DGVM.

Set	Spin-up atmospheric forcing	Spin-up time
S1	one-year atmospheric observations from 1960 to 1999	400 yr
S2	Climatological mean of 1960–1999	400 yr
S3	repeated 1960–1999 interannual forcing	800 yr

years for various spin-up forcings, which are the shortest among all regions. In WM, the periods are about 100 years for most cases, but about 500 and 400 years for S3 and some S1 runs, respectively. Furthermore, in the other five regions, vegetation composition and structure stop evolving after 200–400 years for S1 and S2, and 300–800 years for S3. Hence, after 400 years for S1 and for S2 and after 800 years for S3, the vegetation composition and carbon pools approach equilibrium for all selected regions and spin-up forcings.

4.   Results analysis

Figures 2 and 3 show the mean and standard deviation of the initial and simulated FCs based on various spin-up forcings. Only the three main PFTs are shown, which have the largest averaged FCs of three grid cells in 40 simulation years from the 42 initial conditions. The three lines in each figure represent the simulations of three grid cells in a climate region. The standard deviations of ensemble members are used to assess the impact of spin-up forcing on FC simulations. In Fig. 3, the larger the standard deviation is, the stronger the spin-up forcing affects the simulated FC; the slower the standard deviation decreases, the slower the discrepancy in initial FCs decays and the simulated FCs converges.

4.1   *Tropical rainforest climate region* (*TR*) *and wet temperate climate region* (*WM*)

In TR, only tropical broadleaf evergreen trees (BET Tropical), tropical broadleaf deciduous trees (BDT Tropical), and C4 grasses are present (Figs. 2a–c). In WM, the three main PFTs are temperate broadleaf evergreen trees (BET Temperate), temperate broadleaf deciduous trees (BDT Temperate), and temperate needleleaf evergreen trees (NET Temperate) (Figs. 2j–l). The sum of the FCs of tree PFTs is roughly 95% (the maximum allowed in CLM-DGVM), and no bare soil is present in these two climate regions due to the moist and mild climate characteristics. The discrepancy in initial FCs, which represents the long-term accumulative response of vegetation to different climate anomalies in the spin-up processes, is negligible (Figs. 3a–c, j–l). Furthermore, simulated FCs from 1960 to 1999 are insensitive to climate change

for all initial conditions, so the negligible discrepancy in initial FCs is maintained in the subsequent simulation stage. Thus, in the two regions, the impact of spin-up forcing on FC simulation is weak.

In addition, these results indicate that potential vegetation structures in the two regions are stable. In TR, annual total precipitation and annual average temperature from 1960 to 1999 are 2300–3700 mm and 24°C–26°C, respectively. These values are far from the atmospheric conditions of ecosystem-level resilience threshold of the Amazonian rainforest (Cowling et al., 2004). In WM, the insensitivity of FCs to climate change agrees well with the results of Li et al. (2006) concerning the changes of potential vegetation distribution in China under different climate-change scenarios in the 21st century.

4.2   *Other regions*

Unlike TR and WM, in the other five regions, the impact of spin-up forcing on FCs is considerable, because the discrepancy in initial conditions is large and the large discrepancy usually decays slowly (Fig. 3). The discrepancy in initial FCs represents the long-term accumulative response of vegetation to different climate anomalies, so the large discrepancy in initial FCs indicates the non-negligible impact of climate on FCs in these regions.

In addition, the decay speed of discrepancy in FCs depends on the growth timescales of the vegetation types. FCs of different vegetation types (e.g., grasses, trees, and shrubs) have different intrinsic growth timescales. Here, the word "intrinsic" means that only one vegetation type is present in a grid cell. The grass has only leaf and root pools, and hence has fast growth rates. Besides leaf and root pools, trees have sapwood and heartwood pools with medium and slow growth rates, respectively. Shrubs have sapwood and heartwood pools in much smaller proportion to those of trees. Correspondingly, the intrinsic growth timescale of FCs for different vegetation types, in ascending order, are grasses (several years), shrubs (tens of years) and trees (tens to hundreds of years) (Fu et al., 2001; Hughes et al., 2004; Jarlan et al., 2005; Hughes et al., 2006). This is introduced into CLM-DGVM by adopting different calculation schemes for FCs of different vegetation types (see Appendix A).
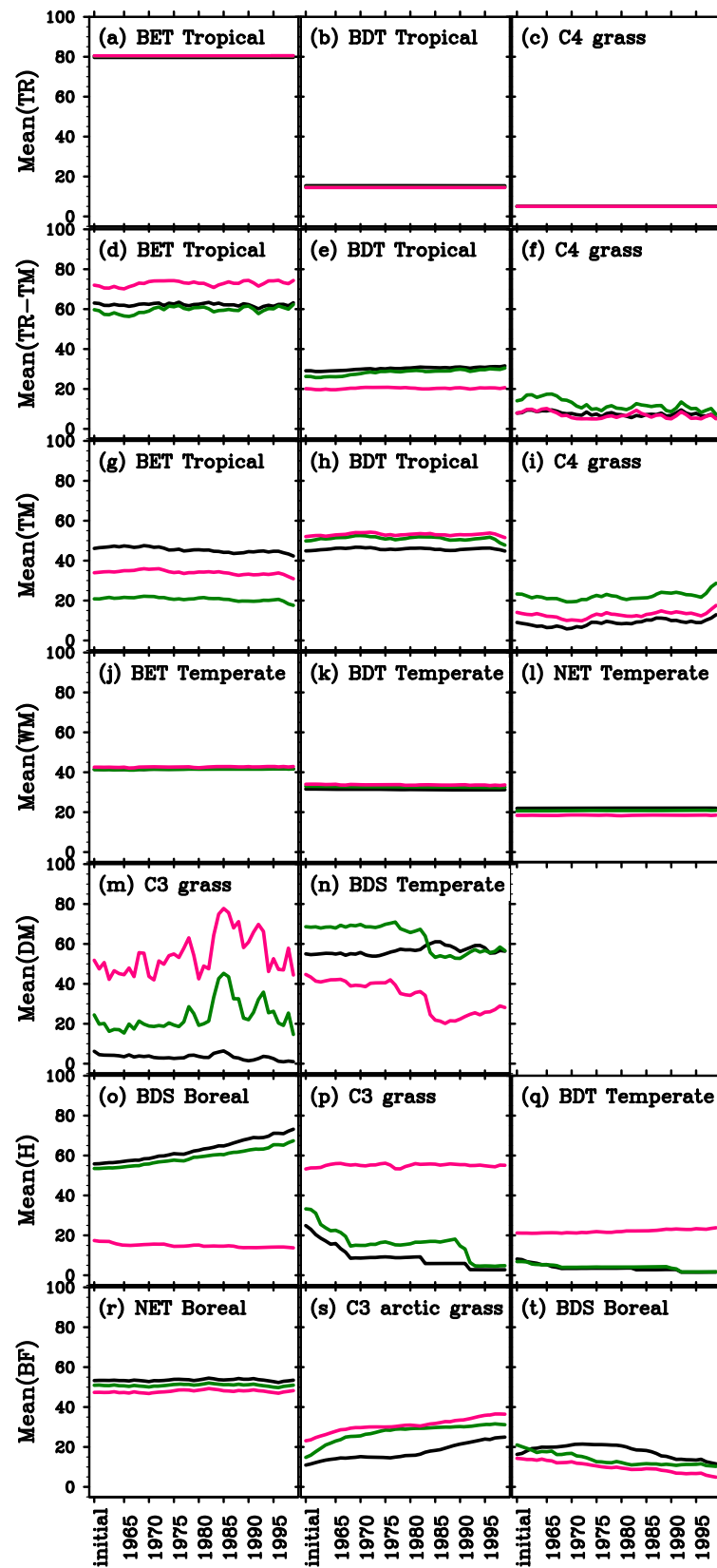
Fig. 2. Means of fractional coverages (FCs, %) from initialization with various spin-up forcings. Only the three main plant functional types (PFTs) in each climate region are shown. Different colors represent different grid cells in each region.
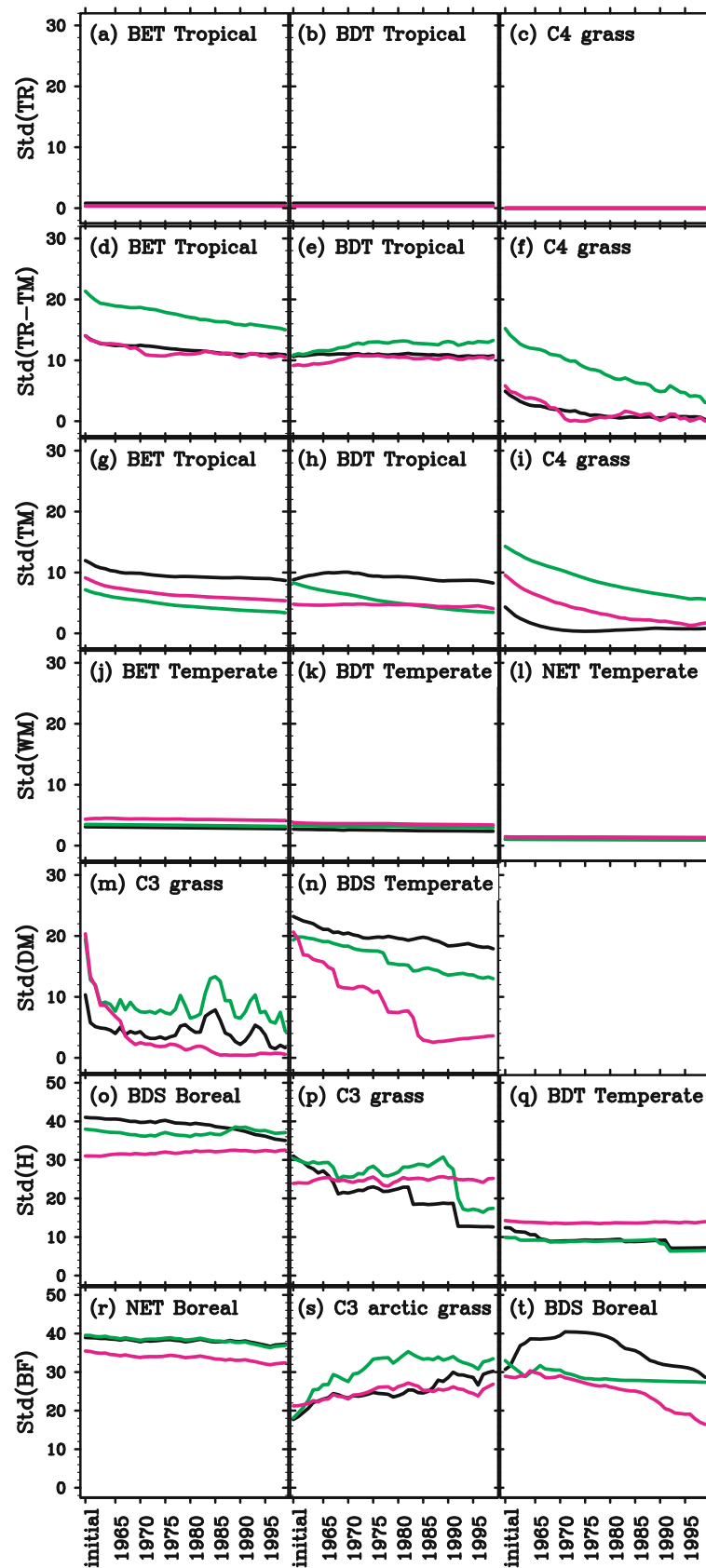
Fig. 3. Same as in Fig. 2, but for standard deviation (Std). Std reflects the discrepancy of simulated FCs.

However, there is usually more than one vegetation type in a grid cell; hence, the growth timescale of FC for a vegetation type may be affected by coexisting vegetation types. With this in mind, we investigate the decay speeds of discrepancies in initial FCs in the five regions as follows.

4.2.1 Tropical monsoon climate region (TM) and TR and TM transition region (TR-TM)

In the two tropical regions, there are only three PFTs: BET Tropical, BDT Tropical, and C4 grass (Figs. 2d–i), with no bare soil. Due to less precipitation and increased seasonality, TM has a lower FC of BET Tropical and higher FCs of BDT Tropical and C4 grass than TR-TM does.

The discrepancies in initial FCs of BET and BDT decay slowly (Figs. 3d–e, g–h) due to their long intrinsic growth timescale. Because the total fractional coverage of natural vegetation (including bare soil) is assumed to be constant in a grid cell (Levis et al., 2004b), the standard deviations of FCs for grasses and trees are always the same (see Appendix B) in the two regions for initial time and each simulation year. For this reason, the discrepancy in the initial FC of C4 grass decays slowly (Figs. 3f and i) due to the slow convergence of the sum of FCs for tree PFTs.

4.2.2 Dry temperate climate region (DM)

In DM, there are only two PFTs: C3 grass and temperate broadleaf deciduous shrub (BDS Temperate) (Figs. 2m and n). Since the influence of atmospheric forcings on the FC of C3 grass is much stronger than that on trees and shrubs (see Appendix A), for all grid cells, the impact of initial conditions on FC of C3 grass decays rapidly (Figs. 3m and n) during the first 1–2 years because the atmospheric forcings are the same for all simulations from various initial conditions.

After that, the decay speeds of discrepancies in initial FCs depend on the shrub/grass ratio. In grid cells with less precipitation (shown by the black and green lines in Figs. 2m and n), the ratio is much higher than that in the other grid cell due to the drought tolerance of BDS Temperate. The discrepancies in initial FCs decay slowly for grasses and shrubs (shown by the black and green lines in Figs. 3m and n), though the intrinsic growth timescale of grasses is short. On the contrary, in a grid cell with more precipitation (shown by the red line in Figs. 2m and n) and a lower shrub/grass ratio than that in the other two grids, the impacts of initial conditions for C3 grass and BDS Temperate decrease more sharply and are negligible after 1968 and 1985, respectively. In the three grid cells, bare soil is present, no light competition between grass

and shrub PFTs occur. Soil wetness and soil temperature may be the bridge for the interdependence between decay speeds of C3 grass and BDS Temperate. In CLM-DGVM, soil wetness and soil temperature are calculated in a vegetation column rather than each PFT, and thus represent the integrated impact of different PFTs; on the other hand, soil wetness and soil temperature can influence FC through affecting NPP and the allocation of NPP (Levis et al., 2004a). The convergence of soil wetness and soil temperature in grid cells indicated by the black and green lines is much slower than that in the grid cell indicated by the red line.

4.2.3 Highland climate region (H)

Boreal broadleaf deciduous shrub (BDS Boreal), C3 grass, and BDT Temperate are the three main PFTs in H (Figs. 2o–q). For the grid cell indicated by a red line with higher temperature and more precipitation, no bare soil is present, and larger FCs of the tree and grass PFTs and smaller FCs of shrubs than those in the other two grid cells can be seen. Similar to TR-TM and TM, FCs from various initial conditions vary faintly, and hence the discrepancy in initial FCs decays slowly.

In the other two grid cells, the temperature is lower, and the precipitation is less. The minimum monthly temperature is lower than $-17°C$ for the climatological mean and is slightly higher than $-17°C$ for some years during 1960–1999. For corresponding S1 simulations, because the 20-year running means of the minimum monthly temperature are lower than the bioclimate limit ($-17°C$ in CLM-DGVM), C3 grass and BDT Temperate are killed in certain years, and these simulations are then close to those with no trees and grasses (shown by the black lines in Figs. 4b and c). Consequently, the impacts of initial conditions on FCs of trees and grasses decrease in a ladder-like fashion (shown by the black and green lines in Figs. 3p and q). However, owing to the slow intrinsic growth rate of shrub PFT on the bare soil, its FC grows slowly (the black lines in Fig. 4a), and thus the impact of initial conditions decays slowly (Fig. 3o).

4.2.4 Boreal forest climate region (BF)

In BF, mainly boreal broadleaf evergreen trees (BET Boreal), C3 arctic grass, and BDS Boreal are present, but some boreal broadleaf deciduous trees (BDT Boreal) and bare soil also occur (Figs. 2r–t). The simulations from different initial conditions can be divided into two categories.

In the first category (shown by the green lines in Fig. 5), the initial soil is wet, and only tree and grass PFTs are present. Trees are the dominant vegetation
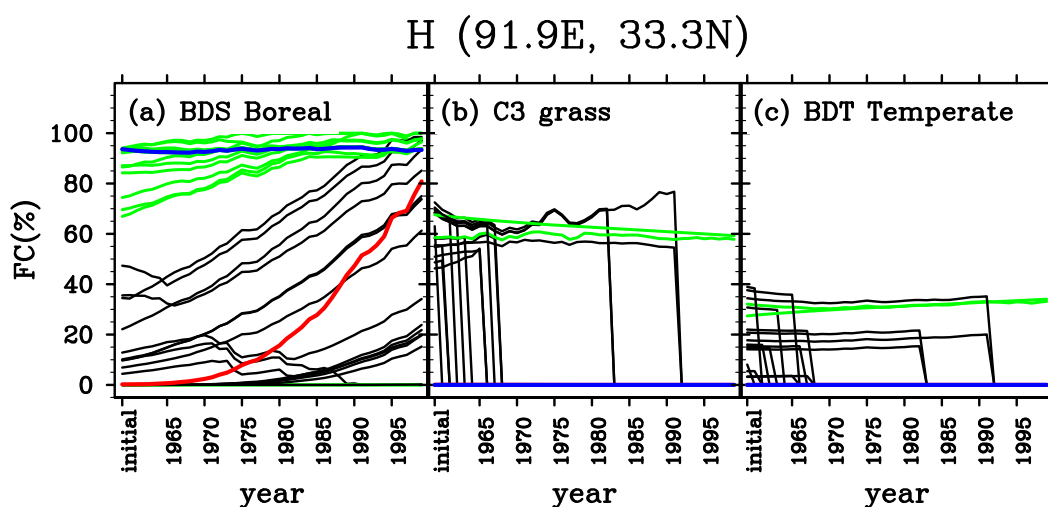
H (91.9E, 33.3N)

Fig. 4. FCs of (a) boreal broadleaf deciduous shrub (BDS Boreal), (b) C3 grass, and (c) temperate broadleaf deciduous tree (BDT Temperate) at a grid cell in highland climate region (H). The red and blue lines indicate the simulations based on S2 and S3 spin-up forcings respectively. The Green and black lines indicate the simulations based on S1 spin-up forcings. Among them, the black lines indicate the simulations in which C3 grass and BDT Temperate are killed because the 20-year running mean of the coldest minimum monthly air temperature is less than the critical value ($-17°$C in CLM-DGVM).

type, and the FC of grass PFT decreases with time and to < 40% after 1975. Because there is no bare soil, the convergence speed of FC for grass PFT relates with that of tree PFTs, as in TR-TM and TM. That is, the influence of initial conditions decreases slowly for both grass and tree PFTs (Figs. 5a and b). In the second category (shown by blue, red, and black lines in Fig. 5), the initial soil is relatively dry, and grasses and shrubs are the main vegetation types. They compete for light in most simulations after 1971 when there is no bare soil. When soil becomes wet, grasses replace the bare soil and the shrubs due to the higher competition rank of grasses in CLM-DGVM (Figs. 5b–d). Grasses tend to be dominant (FC > 70%) in simulations of this category (Fig. 5b). The coexistence of simulations from the two categories leads to the quasi-bifurcation for C3 arctic grass (Fig. 5b) and to an increase in the standard deviation for grass FC with time (Fig. 3s). In the second category, the variation of shrubs' FC is affected by that of grasses and, thus, is relatively rapid (Fig. 5c).

5.   Concluding remarks and discussions

The impact of spin-up forcing in the initialization stage on FC in subsequent simulation stage is investigated in seven climate regions by CLM-DGVM. In TR and WM, where FC simulations from initialization with various commonly used spin-up forcings are nearly the same, the impact of spin-up forcing is neg-

ligible. However, in the other five regions, the impact of spin-up forcing on FC simulations is considerable because the discrepancy in initial FCs is large and the large discrepancy usually decays slowly. The former is due to the long-term accumulation of non-negligible response of vegetation to different climate anomalies. The latter is because trees and shrubs are present in the five regions. The intrinsic growth timescales of FCs for tree and shrub PFTs are long, and the variation of FCs of tree or shrub PFTs can affect that of grass PFTs.

These results suggest that the spin-up forcing usually affects the FCs greatly in regions where two conditions are satisfied: (1) the impact of climate variation on FCs in these regions is non-negligible; (2) trees and/or shrubs are present. First, the discrepancy in initial FCs represents the long-term accumulative response of vegetation to different climate anomalies. The discrepancy is usually large when the first condition is satisfied. Second, the discrepancies in initial FCs of tree and shrub PFTs decrease slowly considering their long intrinsic growth timescales. Although the intrinsic growth timescale of grasses' FC is short, the discrepancy in initial FCs of grass PFTs usually decreases slowly because the variation of FCs of coexistent tree and/or shrub PFTs can affect that of grass PFTs. The two aspects are consistent with ecology knowledge. Therefore, although the two conditions are drawn from only seven regions and CLM-DGVM, they can be adapted on a global scale and to other coupled
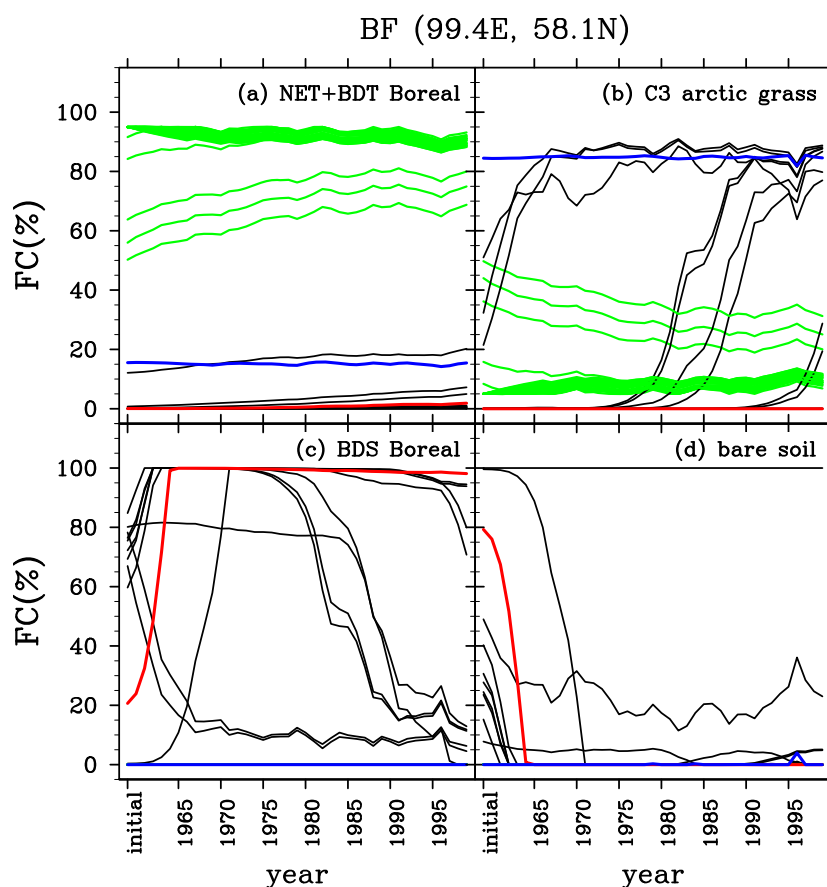
BF (99.4E, 58.1N)

Fig. 5. FCs of (a) boreal needleleaf evergreen tree (NET Boreal) and boreal broadleaf deciduous tree (BDT Boreal), (b) C3 arctic grass, (c) boreal broadleaf deciduous shrub (BDS Boreal) and (d) bare soil at a grid cell in boreal forest climate region (BF). The red and blue lines have the same meanings as Fig. 4. The green and black lines indicate simulations based on S1 spin-up forcings, among which the main vegetation types for the former are trees and grasses and the main vegetation types for the latter are shrubs and grasses due to the wetter soil conditions for the former.

models of DGVM and LSM as long as the models can simulate the response of FC to climate change with some accuracy.

Though only vegetation simulations from the various spin-up forcings are introduced in the present study, the differences in vegetation states will lead to significant differences in land states (e.g. affecting surface albedo, roughness length, soil moisture), and alter the surface fluxes of momentum, heat, carbon, and water further. These will be introduced and discussed in another paper.

In general, spin-up forcing for a coupled model of DGVM and LSM is artificially constructed and different from true atmospheric forcings, so spin-up forcing has errors inevitably. How much the spin-up forcing impacts the subsequent vegetation simulation can be evaluated by spinning up the model using various forcings as shown by this study. For regions where the im-

pact is great, the risk that the errors in spin-up forcing in the initialization stage impact the subsequent simulation is high. In these regions, the impact of spin-up forcing must be considered for parameter adjustment in model development. In addition, when the coupled model of LSM and DGVM is used to investigate mechanisms of a physical process in these regions, one must consider whether the uncertainty in spin-up forcing will change his conclusions. Moreover, if one wants to predict or project climate anomalies using a climate system model or an earth system model that includes the coupled model of LSM and DGVM, data assimilation may be useful to optimize the initial condition.

In the present study, the CLM-DGVM simulations are in offline mode. When CLM-DGVM is coupled with Community Atmosphere Model (CAM) or as a component in a Community Climate System Model (CCSM), CLM-DGVM usually needs to spin up to

an equilibrium state before the coupling in order to reduce the computational expenditure (Levis et al., 2004b; Bonan and Levis, 2006; Cook et al., 2008). As shown in previous studies (Xue, 1996; Hahmann and Dickinson, 1997; Lawrence and Slingo, 2004; Osborne et al., 2004), vegetation has a direct impact on climate over a wide range of time and space scales through physical, chemical, and biological processes that affect planetary energetics, the hydrological cycle, and atmospheric composition. Furthermore, the differences in vegetation and climate simulations from various spin-up forcings may even be magnified by the positive feedback between them in many regions, such as the Amazon basin, the Sahel, and high-latitude regions (Charney, 1975; Pielke et al., 1998, Zeng et al., 1999; Brovkin et al., 2003; Levis et al., 2004b; Cowling et al., 2004; Kim and Wang, 2005; Cook et al., 2008; Bonan, 2008). Therefore, for regions where the impact of spin-up forcing on vegetation simulation is large, risk that errors in spin-up forcings affect the simulation results of CAM-CLM-DGVM and CCSM is high.

APPENDIX A

Representing Growth Timescales for Fractional Coverages of Vegetation Types in CLM-DGVM

In the CLM-DGVM, grasses have only leaf and root carbon pools with 1 and 2 years longevity respectively. Besides leaves and roots, both trees and shrubs have sapwoods, whose longevity is 20 years, and heartwoods, whose carbon pools vary much slower than those of sapwoods. However, the proportion of sapwood and heartwood for shrubs is much smaller than that for trees. Intrinsic growth timescales for fractional coverages (FCs) of different vegetation types (trees, shrubs, and grasses) are different. This is introduced in CLM-DGVM by different calculation schemes of fractional coverage relative to the naturally vegetated land-unit area (FCV) for different vegetation types in the allocation process when FCV is updated at the end of each year.

For tree and shrub PFTs, FCV is calculated by

$$\text{FCV} = PA_c , \tag{A1}$$

where P is the population density (the number of individuals per m^2 naturally vegetated land-unit area), and

$$A_c = k_{\text{allom1}} \left[\frac{4(C_{\text{sapwood}} + \Delta C_{\text{sapwood}} + C_{\text{heartwood}})}{\rho_{\text{wooden}} \pi k_{\text{allom2}}} \right]^{\frac{k_{\text{rp}}}{2 + k_{\text{allom3}}}} \tag{A2}$$

is the average individual's crown area. When the NPP is non-negative in the current year, P is equal to the population density updated at the end of the previous year. In Eq. (A2), k_{allom1}, k_{allom2}, k_{allom3}, and k_{rp} are allometric coefficients; ρ_{wooden} is the density for woody plants; and C_{sapwood} and $C_{\text{heartwood}}$ represent carbon pools in sapwood and heartwood, respectively, that are adjusted slightly in the turnover process in the current year with their sum the same as the values in the end of the previous year. $\Delta C_{\text{sapwood}}$ is the year's biomass increment for sapwood with the proportion of annual net primary production (NPP) which is directly affected by climate. For trees and shrubs, after carbon accumulation for sapwood and especially heartwood in the spin-up stage, $C_{\text{heartwood}} \gg C_{\text{sapwood}} \gg \Delta C_{\text{sapwood}}$, so A_c varies slowly. Therefore, the intrinsic growth timescales for trees and shrubs are long. In CLM-DGVM, for shrubs, because of the low LAI, the photosynthesis level is low and, hence, biomass increment is small (Levis et al., 2004a; Zeng et al., 2008). Moreover, compared with trees, shrubs have a high percentage of leaves and roots and a low percentage of sapwood and heartwood in the allocation of the biomass increment. Consequently, $\Delta C_{\text{sapwood}}$ of shrubs is small and closer to the C_{sapwood} loss ($C_{\text{sapwood}}/20$) in turnover processes, compared with trees. This leads to a larger ratio of $\Delta C_{\text{sapwood}}/C_{\text{sapwood}}$ for shrubs than for trees. Because the turnover ratio of C_{sapwood} to heartwood is not PFT-dependent, the ratios of $C_{\text{sapwood}}/C_{\text{heartwood}}$ are nearly the same for shrubs and trees. For these reasons, shrubs have a higher ratio of $\Delta C_{\text{sapwood}}/(C_{\text{heartwood}} + C_{\text{sapwood}})$ and, hence, shorter intrinsic growth timescale of FCV than trees do. Except for the cases when trees and shrubs cannot survive due to negative NPP or because a 20-year running mean of the coldest minimum monthly air temperature is lower than a corresponding critical values, the adjustment of FCV for trees and shrubs is small and does not affect the long intrinsic growth timescale of the FCV of tree and shrub PFTs.

For grasses, FCV is calculated by

$$\text{FCV} = 1 - e^{-0.5C_{\text{leaf}}A_{\text{sl}}}, \qquad \text{(A3)}$$

where A_{sl} is specific leaf area and is a PFT-dependent constant; living carbon in leaf, C_{leaf}, enters above-ground litter pools totally in turnover process and then is reset in the allocation process each year. The fast response of C_{leaf} to climate leads to the short intrinsic growth time of FCV for the grass PFT.

Because the naturally vegetated land-unit area is constant in CLM-DGVM, the intrinsic growth timescales of FCs for trees, shrubs, and grasses in a grid cell are equal to those of their FCV.

APPENDIX B

For DGVMs (e.g. CLM-DGVM), the total fractional coverage of natural vegetation (including the bare soil) in a grid cell (i, j) is generally assumed to be constant. That is,

$$\text{FC}_{\text{tree},i,j} + \text{FC}_{\text{grass},i,j} + \text{FC}_{\text{shrub},i,j} + \text{FC}_{\text{bare},i,j} = \text{Const}, \qquad \text{(B1)}$$

where $\text{FC}_{\text{tree},i,j}, \text{FC}_{\text{grass},i,j}, \text{FC}_{\text{shrub},i,j}$, and $\text{FC}_{\text{bare},i,j}$ are fractional coverage for trees, grasses, shrubs, and bare soil. In TM and TR-TM, there are no shrubs and bare soil, so

$$\text{FC}_{\text{tree},i,j} + \text{FC}_{\text{grass},i,j} = \text{Const}, \qquad \text{(B2)}$$

and then

$$\text{FC}_{\text{tree},i,j} = \text{Const} - \text{FC}_{\text{grass},i,j}. \qquad \text{(B3)}$$

According to the characteristics of the standard deviation (std), we can derive that

$$\text{std}(\text{FC}_{\text{tree}}, i) = \text{std}(\text{Const} - \text{FC}_{\text{grass}}, i) = \text{std}(\text{FC}_{\text{grass}}, i). \qquad \text{(B4)}$$

REFERENCES

Arora, V. K., 2003: Simulating energy and carbon fluxes over winter wheat using coupled land surface and terrestrial ecosystem models. *Agricultural and Forest Meteorology*, **118**, 21–47.

Betts, R. A., P. M. Cox, S. E. Lee, and F. I. Woodward, 1997: Contrasting physiological and structural feedbacks in climate change simulations. *Nature*, **387**, 796–799.

Bonan, G. B., 2008: Forests and climate change: Forcings, feedbacks, and the climate benefits of forests. *Science*, **320**, 1444–1449.

Bonan, G. B., and S. Levis, 2006: Evaluating aspects of the community land and atmosphere models (CLM3 and CAM3) using a dynamic global vegetation model. *J. Climate*, **19**, 2290–2301.

Bonan, G. B., S. Levis, L. Kergoat, and K. W. Oleson, 2002a: Landscapes as patches of plant functional types: An integrating concept for climate and ecosystem models. *Global Biogeochemical Cycles*, **16**, 1–23.

Bonan, G. B., K. W. Oleson, M. Vertenstein, S. Levis, X. Zeng, Y. Dai, R. E. Dickinson, and Z. L. Yang, 2002b: The land surface climatology of the Community Land Model coupled to the NCAR Community Climate Model. *J. Climate*, **15**, 3123–3149.

Bonan, G. B., S. Levis, S. Sitch, M. Vertenstein, and K. W. Oleson, 2003: A dynamic global vegetation model for use with climate models: Concepts and description of simulated vegetation dynamics. *Global Change Biology*, **9**, 1543–1566.

Brovkin, V., S. Levis, M. F. Loutre, M. Crucifix, M. Claussen, A. Ganopolski, C. Kubatzki, and V. Petoukhov, 2003: Stability analysis of the climate-vegetation system in the northern high latitudes. *Climate Change*, **57**, 119–138.

Charney, J., 1975: Dynamics of deserts and droughts in the Sahel. *Quarterly Journal of Royal Meteorological Society*, **101**, 193–202.

Chen, M, 2008: Couple the common land model with the dynamic global vegetation model. M. S. thesis, Institute of Atmospheric physics, Chinese Academy of Sciences, 43pp. (in Chinese)

Cook, B. I., G. B. Bonan, S. Levis, and E. Epstein, 2008: Rapid vegetation responses and feedbacks amplify climate model response to snow cover changes. *Climate Dyn.*, **30**, 391–406.

Cowling, S., and Coauthors, 2004: Contrasting simulated past and future responses of Amazonian forest to atmospheric change. *Philosophical Transactions of the Royal Society B: Biological Sciences*, **359**, 539–547.

Cox, P., 2001: Description of the "TRIFFID" Dynamic Global Vegetation Model. Hadley Center Techical Note 24, 16pp.

Cramer, W., and Coauthors, 2001: Global response of terrestrial ecosystem structure and function to CO_2 and climate change: Results from six dynamic global vegetation models. *Global Change Biology*, **7**, 357–373.

Dai, Y., and Coauthors, 2003: The common land model. *Bull. Amer. Meteor. Soc.*, **84**, 1013–1023.

Dai, Y., R. E. Dickinson, and Y. P. Wang, 2004: A two-big-leaf model for canopy temperature, photosynthesis, and stomatal conductance. *J. Climate*, **17**, 2281–2299.

Essery, R., M. Best, R. Betts, P. M. Cox, and C. Taylor, 2001: Explicit representation of subgrid heterogeneity in a GCM land-surface scheme. *Climate Dyn.*, **4**, 530–543.

Fisher, R., cited 2008: Title of subordinate document. ED-JULES progress. [Available online at http://www.jchmr.org/jules/pdf/2008_Fisher_ED.pdf.]

Foley, J. A., I. C. Prentice, N. Ramankutty, S. Levis, D. Pollard, S. Sitch, and A. Haxeltine, 1996: An integrated biosphere model of land surface processes, terrestrial carbon balance, and vegetation dynamics.

Global Biogeochemical Cycles, **10**, 603–628.

Fu, B. J., and Coauthors, 2001: *Theory and Application of Landscape Ecology*. Science Press, Beijing, China, 303pp. (in Chinese)

Hahmann, A. N., and R. E. Dickinson, 1997: RCCM2-BATS model over tropical South America: Applications to tropical deforestation. *J. Climate*, **10**, 1944–1964.

Hughes, J. K, P. J. Valdes, and R. A. Betts, 2004: Dynamical properties of the TRIFFID dynamic global vegetation model. Hadley Centre Technical Note 56, 23pp.

Hughes, J. K., P. J. Valdes, and R. Betts, 2006: Dynamics of a global-scale vegetation model. *Ecological Modelling*, **198**, 452–462.

Jarlan, L., Y. M. Tourre, E. Mougin, N. Philippon, P. Mazzega, 2005: Dominant patterns of AVHRR NDVI interannual variability over the Sahel and linkages with key climate signals (1982–2003). *Geophys. Res. Lett.*, **32**, doi: 10.1029/2004GL021841.

Kim, Y., and G. Wang, 2005: Modeling seasonal vegetation variation and its validation against Moderate Resolution Imaging Spectroradiometer (MODIS) observations over North America. *J. Geophys. Res.*, **110**, doi: 10.1029/2004JD005436.

Krinner, G., and Coauthors, 2005: A dynamic global vegetation model for studies of the coupled atmosphere-biosphere system. *Global Biogeochemical Cycles*, **19**, doi: 10.1029/2003GB002199.

Köhler, P., F. Joos, S. Gerber, and R. Knutti, 2005: Simulated changes in vegetation distribution, land carbon storage, and atmospheric CO_2 in response to a collapse of the North Atlantic thermohaline circulation. *Climate Dyn.*, **25**, 689–708.

Kucharik, C. J., and Coauthors, 2000: Testing the performance of a dynamic global ecosystem model: Water balance, carbon balance and vegetation structure. *Global Biogeochemical Cycles*, **14**, 795–825.

Lawrence, D., and J. Slingo, 2004: An annual cycle of vegetation in a GCM. Part I: implementation and impact on evaporation. *Climate Dyn.*, **22**, 87–105.

Levis, S., G. B. Bonan, M. Vertenstein, and K. W. Oleson, 2004a: The Community Land Model's dynamic global vegetation model (CLM-DGVM): Technical description and user's guide. NCAR Techical Note TN-459+IA, 50pp.

Levis, S., G. B. Bonan, and C. Bonfils, 2004b: Soil feedback drives the Mid-Holocene North African monsoon northward in fully coupled CCSM2 simulations with a dynamic vegetation model. *Climate Dyn.*, **23**, doi: 10.1007/s00382-004-0477-y.

Li, Y., M. Cao, and K. Li, 2006: Climate-induced changes in the vegetation pattern of China in the 21st centrury. *Ecological Research*, **21**, 912–919.

Liang, M. L., and Z. H. Xie, 2008: Improving the vegetation dynamic simulation in a land surface model by using a statistical-dynamic canopy interception scheme. *Adv. Atmo. Sci.*, **25**, 610–618.

Liu, S. F., 2007: Skill validation of an atmosphere-land-

vegetation coupled model and the analysis of its coupling strength. Ph. D. dissertation, Institute of Atmospheric physics, Chinese Academy of Sciences, 185pp.

Morales, P., H. Hickler, D. P. Rowell, B. Smith, and M. T. Sykes, 2007: Changes in European ecosystem productivity and carbon balance driven by regional climate model output. *Global Change Biology*, **13**, 108–122.

Oleson, K. W., and Coauthors, 2008: Improvements to the Community Land Model and their impact on the hydrological cycle. *J. Geophys. Res.*, **113**, G01021, doi: 10.1029/2007JG000563.

Osborne, T. M., D. M. Lawrence, J. M. Slingo, A. J. Challinor, and T. R. Wheeler, 2004: Influence of vegetation on the local climate and hydrology in the tropics: Sensitivity to soil parameters. *Climate Dyn.*, **23**, 45–61.

Peel, M. C., B. L. Finlayson, and T. A. McMahon, 2007: Updated world map of Köppen-Geiger climate classification. *Hydrology and Earth System Sciences Discussions*, **4**, 439–473.

Pielke, R. A., R. Avissar, M. Raupach, A. J. Dolman, X. Zeng, and A. S. Denning 1998: Interactions between the atmosphere and terrestrial ecosystems: Influence on weather and climate. *Global Change Biology.*, **4**, 461–475.

Qian, T., A. Dai, K. E. Trenberth, and K. W. Oleson, 2006: Simulation of global land surface conditions from 1948 to 2004. Part I: Forcing data and evaluations. *Journal of Hydrometeorology*, **7**, 953–975.

Rodell, M., P. R. Houser, A. A. Berg, and J. S. Famiglieti, 2005: Evaluation of 10 methods for initializating a land surface model. *Journal of Hydrometeorology*, **6**, 146–155.

Sato, H., A. Itoh, and T. Kohyama, 2007: SEIB-DGVM: A new Dynamic Global Vegetation Model using a spatially explicit individual-based approach. *Ecological Modelling*, **200**, 279–307.

Sitch, S., and Coauthors, 2003: Evaluation of ecosystem dynamics, plant geography and terrestrial carbon cycling in the LPJ dynamic global vegetation model. *Global Change Biology*, **9**, 161–185, doi: 10.1046/j.1365-2486.2003.00569.x.

Xue, Y., 1996: The impact of desertification in the Mongolian and the Inner Mongolian grassland on the regional climate. *J. Climate*, **9**, 2173–2189.

Yang, Z. L., R. E. Dickinson, A. Henderson-Sellers, and A. J. Pitman, 1995: Preliminary study of spin-up processes in land surface models with the first stage of project for intercomparison of Land Surface Parameterization Schemes Phase 1(a). *J. Geophys. Res.*, **100**, 16553–16578.

Zeng, N., J. Neelin, K. M. Lau, and C. Tucker, 1999: Enhancement of interdecedal climate variability in the Sahel by vegetation interaction. *Science*, **286**, 1537–1540.

Zeng, N., A. Mariotti, and P. Wetzel, 2005: Terrestrial mechanisms of interannual CO_2 variability.

Global Biogeochemical Cycles, **19**, doi: 10.1029/2004-GB002273.

Zeng, Q. C., and Coauthors, 2008: Research on the earth system dynamic model and some related numerical simulations. *Chinese J. Atmos. Sci.*, **32**, 653–690. (in Chinese)

Zeng, X., 2001: Global vegetation root distribution for land modeling. *Journal of Hydrometeorology*, **2**, 525–530.

Zeng, X. D., X. Zeng, and M. Barlage, 2008: Growing temperate shrubs over arid and semiarid regions in the NCAR Dynamic Global Vegetation Model (CLM-DGVM). *Global Biogeochemical Cycles*, **22**, doi: 10.1029/2007GB003014.

Zeng, X. D., 2010: Evaluating the dependence of vegetation on climate in an improved dynamic global vegetation model (CLM3.0-DGVM). *Adv. Atmos. Sci.*, **27**, 977–991, doi: 10.1007/s00376-009-9186-0.